NANO LETTERS

2007
Vol. 7, No. 11
3483−3488

Correlating Dynamics and Selectivity in Adsorption of Semiconductor Nanocrystals onto a Self-Organized Pattern

Xiaodong Chen,[†,‡] Michael Hirtz,[†] Andrey L. Rogach,[§] Dmitri V. Talapin,[||] Harald Fuchs,[†] and Lifeng Chi*[,†]

Physikalisches Institut, Westfälische Wilhelms-Universität Münster, Wilhelm-Klemm-Strasse 10, 48149 Münster, Germany, Center for Nanotechnology (CeNTech), Gievenbeckweg 11, 48149 Münster, Germany, Physics Department and Center of Nanoscience (CeNS), Ludwig-Maximilians-Universität München, 80799 München, Germany, and The Molecular Foundry, Lawrence Berkeley National Laboratory, Berkeley, California 94720

Received August 16, 2007; Revised Manuscript Received September 19, 2007

ABSTRACT

Selective adsorption of semiconductor nanocrystals onto an organic self-organized pattern shows a time-dependent behavior. By studying the wetting behavior of delivered solvent (1-phenyloctane) on a lipid self-organized pattern and determining the adhesion energy between semiconductor nanocrystals and substrate, we obtain a correlation between dynamics and selectivity in adsorption of semiconductor nanocrystals onto the pattern by constructing a potential energy landscape. Two consecutive steps for selective adsorption of nanocrystals onto the self-organized pattern have been established: the first one is the molecule exchange of 1-phenyloctane and lipid molecules to form the adsorption sites for nanocrystals, and the second one is the adsorption of nanocrystals onto the adsorption sites due to the strong interaction between nanocrystals and substrate.

Significant advancement has been made in the synthesis of semiconductor nanocrystals (NCs) with excellent control over particle size and shape.[1−3] A grand challenge, however, resides in assembling individual NCs in higher level organized functional assemblies, which would significantly impact their possible applications in photonic and optoelectronic devices.[4−6] Patterning of NCs is usually achieved by directed assembly on different templates fabricated by top-down techniques, such as photolithography,[7] e-beam lithography,[8] soft lithography,[9] dip-pen lithography,[10] constructive nanolithography,[11] and nanoimprinting lithography.[12] On the other side, the use of bottom-up techniques based on self-assembly phenomena provides a useful alternative to pattern NCs on a large scale because of their simplicity and compatibility with heterogeneous integration processes.[13,14] There are two strategies for the latter: (i) assembly of NCs in to self-assembled patterns on suitable templates,[15,16] and (ii) fabrication of NC arrays with the help of specific physical phenomena, such as fingering instability[17] and the stick−slip motion of a water meniscus.[18]

Recently, we introduced a simple method for patterning semiconductor NCs into periodic lateral structures over large areas (several cm^2) within a few minutes based on multistep self-assembly processes on different length scale.[19] The procedure is remarkably controllable, high-yielding, and easy to implement. Furthermore, we generated hierarchical luminescent patterns based on specific properties of CdSe NCs and dyes in response to light irradiation.[20] To fully understand the mechanism of selective deposition of NCs and expand their potential application, several important questions, which include the controllability of the NCs deposition and the driving force for the selective deposition, need to be addressed. Herein we addressed the mechanism of specific NC adsorption by construction of a potential energy landscape to permit a qualitative correlation between dynamics and selectivity of NC deposition based on the experimental results.

* Corresponding author. E-mail: chi@uni-muenster.de.
[†] Physikalisches Institut, Westfälische Wilhelms-Universität Münster and Center for Nanotechnology (CeNTech).
[‡] Present address: Department of Chemistry, Northwestern University, Evanston, IL 60208.
[§] Physics Department and Center of Nanoscience (CeNS), Ludwig-Maximilians-Universität München.
[||] The Molecular Foundry, Lawrence Berkeley National Laboratory.

10.1021/nl072069b CCC: $37.00
Published on Web 10/03/2007

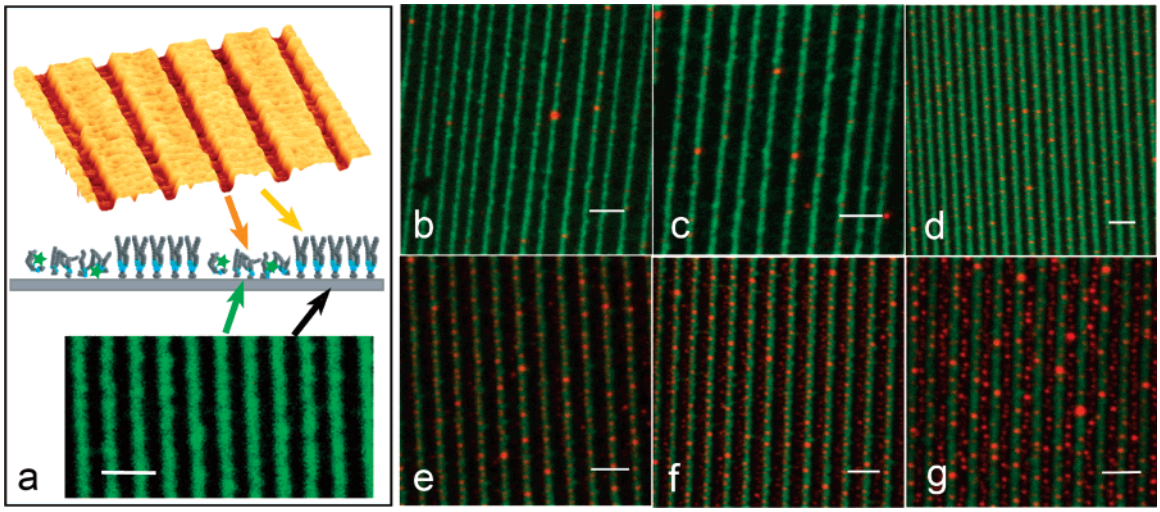

Figure 1. (a) Morphology (top) and CLSM (bottom) images of DPPC stripe patterns, which are composed of expanded DPPC and condensed DPPC alternatively. (b−g) A series of CLSM images of CdSe NCs adsorbed on self-organized luminescent lipid patterns depending on the duration of contact between NCs in 1-phenyloctane and the patterns: (b) 0.5 min, (c) 1 min, (d) 5 min, (e) 10 min, (f) 20 min, and (g) 40 min. (Bar = 2 μm.) The images are obtained by merging images of BODIPY luminescent stripe patterns (λ_{ex} = 488 nm, detection range 500−550 nm) and CdSe NCs arrays (λ_{ex} = 488 nm, detection range 650−700 nm).

To address the question of the controllability of the NCs deposition, we studied deposition of NCs depending on duration of the contact between NCs dispersed in 1-phenyloctane and the lipid-based patterns. Similar to the published procedure,[20] a droplet of ~0.1 mg/mL CdSe NCs (5.5 nm diameter, synthesized according to the previously published procedure[21]) in 1-phenyloctane was dripped on a well-aligned luminescent lipid pattern, which was obtained by transferring the monolayer of L-α-dipalmitoyl-phosphatidylcholine (DPPC) and 2-(4,4-difluoro-5-methyl-4-bora-3a,4a-diaza-s-indacene-3-dodecanoyl)-1-hexadecanoyl-*sn*-glycero-3-phosphocholine (BODIPY) (0.5 mol %) onto a mica surface by means of a Langmuir−Blodgett (LB) technique due to a substrate-mediated microphase separation and a periodic oscillation of the meniscus at the three-phase contact line.[22] As was demonstrated before,[22] green-emitting stripes of the lipid pattern are formed by expanded DPPC enriched in BODIPY (termed expanded DPPC channel), while the dark stripes are mainly composed of condensed DPPC (termed condensed DPPC stripe), shown in Figure 1a. After some time of wetting, the droplet was sucked up by a pipet or filter paper, and the samples were characterized by confocal laser scanning microscopy (CLSM). Panels b−g of Figure 1 show a series of CLSM images obtained upon increasing wetting time of NCs dispersed in 1-phenyloctane on the pattern surface. For a short time of wetting (less than 10 min), most NCs tend to assemble into the expanded DPPC channels, confirmed by the results of atomic force microscopy (AFM) measurement (Figure 2a). However, when the wetting time is increased to 20 min, CdSe NCs are not only assembled within the expanded DPPC channels but also appear on top of condensed DPPC stripes, which is demonstrated by AFM measurement (Figure 2b) and CLSM measurement (Figure 1e). Upon further increase of the wetting time, more NCs tend to assemble on top of the condensed DPPC stripe (Figure 1g). Therefore, we hypothesize that the selective deposition of NCs on the self-organized lipid pattern strongly depends on the wetting time, as schematically presented in Figure 2c. It should be noted here that the selection of solvent is the trick in our present system; that is, (1) CdSe NCs should be well-dispersed in the selected solvent and (2) the selected solvent cannot dissolve the DPPC, otherwise it would destroy DPPC pattern quickly. So far, hexadecane is another suitable solvent for our system and shows similar

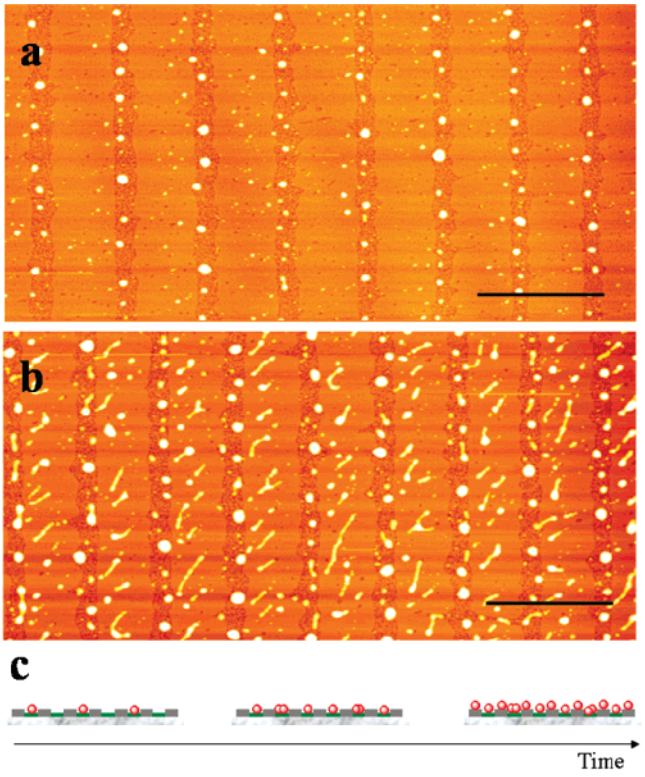

Figure 2. AFM images of CdSe NCs on the self-organized lipid patterns. After (a) 5 min and (b) 20 min of wetting with NCs solution. Scale bar = 2 μm. (c) Schematics of selective adsorption of CdSe NCs onto patterns depending on the deposition time.

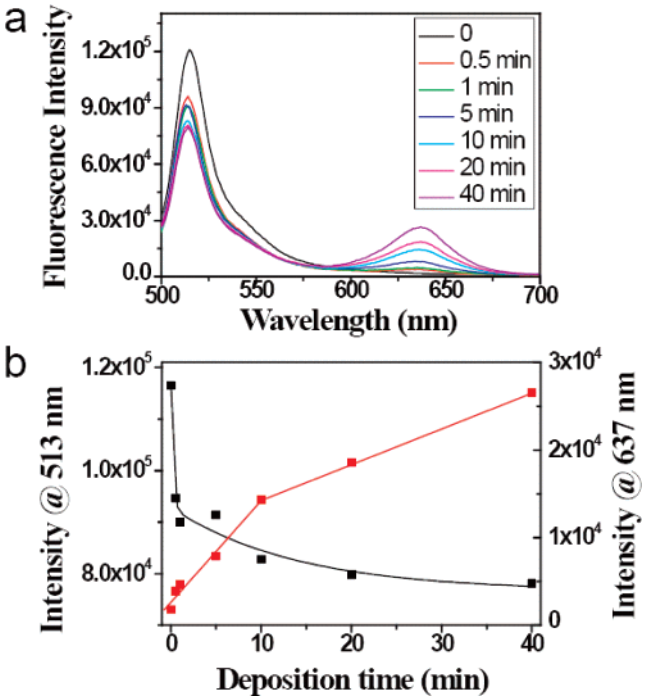

Figure 3. Tunable deposition of CdSe NCs on the self-organized DPPC pattern by adjusting the wetting time. (a) A series of fluorescence spectra depending on the deposition time. (b) The fluorescence intensity at 513 nm (characteristic peak of BODIPY) and 637 nm (characteristic peak of CdSe NCs) depending on the deposition time.

behavior to 1-phenyloctane, but there is not much difference in selectivity and controllability of adsorption.

Fluorescence spectra shown in Figure 3 further confirm selective deposition of CdSe NCs on the DPPC pattern depending on the duration of contact between the NCs in 1-phenyloctane and the patterns. The fluorescence intensity at 513 nm (characteristic peak of BODIPY) decreases with increasing the wetting time (Figure 3b, black curve), which suggests that BODIPY molecules exchange with the solvent during the contact between NCs in 1-phenyloctane solution and lipid patterns, so that some BODIPY molecules are detached from the patterns when the droplet was sucked up by the pipet. The fluorescence intensity at 637 nm, which is the characteristic peak of CdSe NCs, increases with the progression of the wetting time (Figure 3b, red curve). The slope of the line for fitting the short wetting time (less than 10 min) is larger than that of the long time (more than 10 min), which suggests that the kinetic behavior for short time and long time is different, or in other words, the kinetic behavior for NCs assembling onto the expanded DPPC channel is different from those assembling onto the condensed DPPC stripe if we consider Figure 1 and Figure 3 together. From the slope of the fitting curve, it is evident that the depositing speed for NCs on the expanded DPPC channel is faster than that on the condensed DPPC stripe. Thus, there are two questions: (i) What is the driving force for the deposition of NCs onto the DPPC pattern? (ii) Why are the kinetic behaviors of NCs depositing on the expanded DPPC channel and on the condensed DPPC stripe different?

To address the above-mentioned questions, we first studied the wetting behavior of a pure solvent, 1-phenyloctane, on the DPPC pattern. Figure 4a shows the AFM image of a pure DPPC pattern before 1-phenyloctane is added onto the surface. For the DPPC pattern, the channels are composed of the expanded DPPC molecules (green color in Figure 4a), while the stripes are composed of the condensed DPPC molecules (blue color in Figure 4a), with some holes in the stripe being filled with the expanded DPPC molecules. The height difference between the expanded DPPC channel and the condensed DPPC stripe is ~0.9 nm. When the DPPC pattern is wetted by 1-phenyloctane for 2 min, some small holes appear in channels, and the numbers of holes in stripes also increase (Figure 4b). If we further increase the wetting time, the number of holes in channels and stripes keeps increasing (Supporting Information). We measured the depth of the holes from the height profile of AFM images to clarify the nature of the holes. The depth of holes in the expanded DPPC channel is ~0.8 nm, which is similar to the length of an expanded DPPC molecule. On the other hand, two different depths of holes have been found in the condensed DPPC stripe: 0.9 nm which is obviously same to the height difference between the channel and the stripe, and 1.7 nm which corresponds to the level of holes in the channel. Considering the length of the DPPC molecule being ~2 nm, the bottom of the holes in the channels is attributed to mica support. Similarly, the holes in the stripes correspond to expanded DPPC for the shallow holes (0.9 nm) and to mica for the deep holes (1.7 nm). In color coding of the AFM image in Figure 4b, the blue region is condensed DPPC, the green region is expanded DPPC, and the yellow region is mica.

Furthermore, we systematically analyzed the area coverage of holes in stripes and channels depending on the wetting time (AFM images shown in the Supporting Information) considering three different types of area coverage: mica in channels, expanded DPPC in stripes, and mica in stripes. The data presented in Figure 4c can be well fitted by the following monoexponential equation

$$C = -A\exp\left(-\frac{t}{\tau}\right) + C_0 \qquad (1)$$

where C is the coverage, A the front factor, τ the lifetime, and C_0 the coverage for the time approaching infinity. From the lifetime, the rate constants $k = 1/\tau$ have been obtained: $0.011 \pm 0.002\ s^{-1}$ (k_1) for expanded DPPC in the stripe, $0.0023 \pm 0.0006\ s^{-1}$ (k_2) for mica in the stripe, and $0.018 \pm 0.002\ s^{-1}$ (k_3) mica in the channel. According to the rate law

$$k = \frac{k_B T}{h}\exp\left(-\frac{\Delta G^{\#}}{k_B T}\right) \qquad (2)$$

with $\Delta G^{\#}$ being activation free energy, and knowing the rate constants already, we can roughly estimate the relative free energy, which has been used to construct relative potential energy landscapes (Figure 5) to reveal the relationship

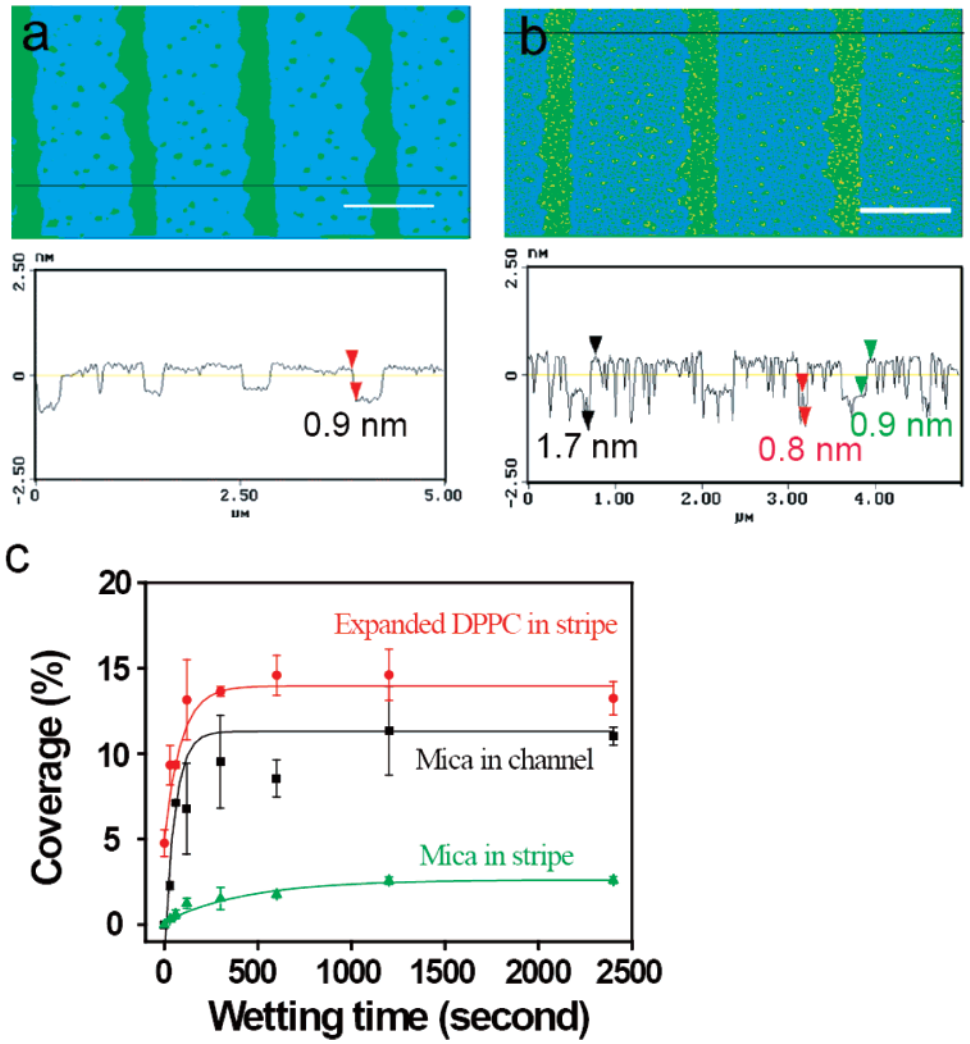

Figure 4. AFM image and corresponding height profile of (a) pure DPPC pattern and (b) 1-phenyloctane on DPPC pattern after 2 min of wetting time. Scale bar = 1 μm. (c) Coverage analysis depending on wetting time.

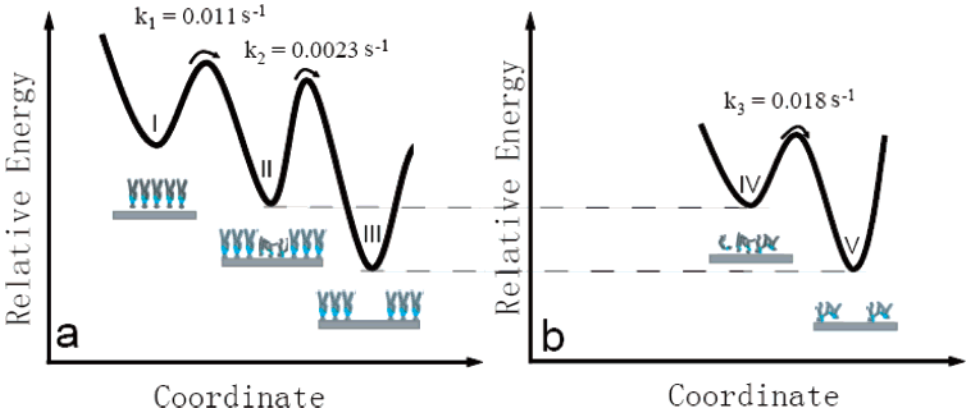

Figure 5. Schematic representation of the potential energy landscapes for the DPPC pattern (a, stripes; b, channels) energetically closer to mica (lower energy) and kinetically closer to mica (smaller barrier to cross). Region I represents the condensed DPPC in stripe, II the expanded DPPC in stripe, III mica in stripe, IV the expanded DPPC in channel, and V mica in channel.

between dynamics and selectivity of NC adsorption in channels and stripes (see later for detailed discussion).

The energy levels for regions denoted as "II' and "IV" (see Figure 5 caption for explanations) are the same, or in other words, thermodynamics is the same, whereas "IV" is kinetically closer to "V" due to the smaller barrier to cross compared with "II". It is interesting to note that the rate constants are different by 1 order of magnitude for transition from II to III (k_2) as compared with transition from IV to V (k_3), although both are from expanded DPPC to mica. This can be understood by considering the relative free movement of DPPC in channels (expanded DPPC phase) and restricted

movement of DPPC in stripes (condensed DPPC phase). The process of wetting the DPPC pattern with 1-phenyloctane can be considered as a "caving" process by exchanging DPPC molecules with 1-phenyloctane. At the very beginning, being kinetically closer to mica (a small barrier to cross), 1-phenyloctane drills holes in the channel (mica in channel). Simultaneously, the holes of expanded DPPC in stripe also appear. On a longer time scale, the holes corresponding to mica in the stripe appear, determined by thermodynamics.

The interaction energy between the substrate and NCs suspended in 1-phenyloctane, which can be approximated as the favorable adhesion energy gained by bringing NCs in a close contact with substrate, provides us with estimation of the selective adsorption of CdSe NCs from 1-phenyloctane solution onto DPPC pattern. This energy may be expressed as[23]

$$E_{ad} = A_{eff}(\gamma_{13} - \gamma_{12} - \gamma_{23}) \quad (3)$$

where A_{eff} is the effective area of contact between NCs and substrate, γ_{13} is the interfacial energy of the NCs-substrate interface, γ_{12} is the interfacial energy of the NC−solvent interface, and γ_{23} is the interfacial energy of the solvent−substrate interface. In formula 3, the effective contact area is $A_{eff} \approx 4\pi Ra$, where a is the measure of range of the forces (usually on the order of molecular dimensions, here, a is taken as ∼1 nm being determined by molecular length of trioctylphosphine oxide, trioctylphosphine, and hexadecylamine which are the organic ligands surrounding the NCs) and R is the radius of the NCs. According to Owens and Wendt,[24] we estimate the interfacial energies of the different interfaces as $\gamma_{NC-phenyloctane} = 1.9$ mJ/m^2, $\gamma_{NC-condensed} = 1.1$ mJ/m^2, $\gamma_{condensed-phenyloctane} = 0.7$ mJ/m^2, $\gamma_{NC-expanded} = 1.3$ mJ/m^2, $\gamma_{expanded-phenyloctane} = 5.0$ mJ/m^2, $\gamma_{NC-mica} = 49.4$ mJ/m^2, and $\gamma_{mica-phenyloctane} = 65.0$ mJ/m^2. (See Supporting Information for detailed calculations) The adhesion energy between NCs and substrate is $E_{ad(NC-condensed)} = -5.2 \times 10^{-19}$ J, $E_{ad(NC-expanded)} = -1.9 \times 10^{-18}$ J, and $E_{ad(NC-mica)} = -6.0 \times 10^{-18}$ J. Comparison of these values indicates that the interaction between NCs and mica is stronger than that between NCs and the expanded DPPC phase (channels) or the condensed DPPC phase (stripes), which suggests that NCs preferentially adsorb onto mica. The adhesion energy between NCs and substrate is also much higher than the thermal energy of NCs ($3/2kT \sim 6.2 \times 10^{-21}$ J) which forces adsorption of NCs on the substrate.

So far, we can completely understand the selective adsorption of CdSe NCs dispersed in 1-phenyloctane onto a DPPC pattern, which is correlated with thermodynamics and kinetics. Because the work of adhesion of 1-phenyloctane on expanded DPPC (62.0 mJ/m^2) is larger than that of 1-phenyloctane on condensed DPPC (53.7 mJ/m^2), 1-phenyloctane preferentially wets expanded DPPC. Moreover, due to the loose stacking of DPPC molecules in the expanded DPPC channel and the work of adhesion of 1-phenyloctane on mica (63.3 mJ/m^2) being larger than that of 1-phenyloctane on expanded DPPC (62.0 mJ/m^2), 1-phenyloctane penetrates into the channel finally approaching the mica substrate by exchanging DPPC molecules with 1-phenyloctane molecules following the potential energy landscapes presented in Figure 5b. During this process, NCs will follow the way of 1-phenyloctane to occupy the holes due to the strong interaction between NCs and mica substrate ($E_{ad(NC-mica)} = -6.0 \times 10^{-18}$ J). On the longer time scale, previously adsorbed NCs will act as nuclei to form NC aggregates in DPPC channels, which results in specific deposition of NCs in the channels of DPPC pattern. According to the potential energy landscapes, for stripes (Figure 5a) the NCs have to traverse two barriers to approach mica, while for channels (Figure 5b) only one barrier, which is the most important reason that NCs selectively deposited in the channels of DPPC pattern at the beginning. However, on an even longer time scale NCs will also deposit onto stripes at places where mica in stripe appear (Figure 5a). This is the reason why the kinetic behavior of NCs depositing onto expanded DPPC channels and onto condensed DPPC stripes is different (Figure 3b).

In summary, based on the experimental results, we have constructed potential energy landscapes in order to reveal correlation between dynamics (thermodynamics and kinetics) and selectivity of NC adsorption onto the self-organized DPPC pattern. The following two-step adsorption mechanism has been established: (1) wetting of 1-phenyloctane on two different DPPC phases (expanded in channels and condensed in stripes) induces the formation of holes preferentially in channels by exchanging 1-phenyloctane molecules with DPPC molecules; (2) NCs follow 1-phenyloctane to occupy the holes due to the strong interaction between NCs and mica substrate, and previously adsorbed NCs act as nuclei to form NC aggregates in the DPPC channels, which results in selective deposition of NCs in channels of DPPC pattern.

Acknowledgment. Financial support of the German−Israeli Foundation and the German Excellence Initiative via the "Nanosystems Initiative Munich (NIM)" is gratefully acknowledged.

Supporting Information Available: Detailed experimental description, a series of AFM images for 1-penyloctane on pure DPPC pattern depending on the wetting time, and parameters obtained by fitting the coverage depending on wetting time to the monoexponential equation, detailed calculation of interfacial energy, adhesion energy, and work of adhesion. This material is available free of charge via the Internet at http://pubs.acs.org.

References

(1) Alivisatos, A. P. *Science* **1996**, *271*, 933−937.
(2) Murray, C. B.; Kagan, C. R.; Bawendi, M. G. *Annu. Rev. Mater. Sci.* **2000**, *30*, 545−610.
(3) Rogach, A. L.; Talapin, D. V.; Shevchenko, E. V.; Kornowski, A.; Haase, M.; Weller, H. *Adv. Funct. Mater.* **2002**, *12*, 653−664.
(4) Crooker, S. A.; Hollingsworth, J. A.; Tretiak, S.; Klimov, V. I. *Phys. Rev. Lett.* **2002**, *89*.
(5) Klein, D. L.; Roth, R.; Lim, A. K. L.; Alivisatos, A. P.; Mceuen, P. L. *Nature* **1997**, *389*, 699−701.
(6) Gao, M. Y.; Sun, J. Q.; Dulkeith, E.; Gaponik, N.; Lemmer, U.; Feldmann, J. *Langmuir* **2002**, *18*, 4098−4102.
(7) Xu, H.; Hong, R.; Lu, T. X.; Uzun, O.; Rotello, V. M. *J. Am. Chem. Soc.* **2006**, *128*, 3162−3163.

(8) Werts, M. H. V.; Lambert, M.; Bourgoin, J. P.; Brust, M. *Nano Lett.* **2002**, *2*, 43−47.
(9) Guo, Q. J.; Teng, X. W.; Rahman, S.; Yang, H. *J. Am. Chem. Soc.* **2003**, *125*, 630−631.
(10) Thomas, P. J.; Kulkarni, G. U.; Rao, C. N. R. *J. Mater. Chem.* **2004**, *14*, 625−628.
(11) Liu, S. T.; Maoz, R.; Sagiv, J. *Nano Lett.* **2004**, *4*, 845−851.
(12) Maury, P.; Escalante, M.; Reinhoudt, D. N.; Huskens, J. *Adv. Mater.* **2005**, *17*, 2718−2723.
(13) Boncheva, M.; Whitesides, G. M. *MRS Bull.* **2005**, *30*, 736−742.
(14) Chen, X. D.; Lenhert, S.; Hirtz, M.; Lu, N.; Fuchs, H.; Chi, L. F. *Acc. Chem. Res.* **2007**, *40*, 393−401.
(15) Haryono, A.; Binder, W. H. *Small* **2006**, *2*, 600−611.
(16) Zhang, L.; Gaponik, N.; Muller, J.; Plate, U.; Weller, H.; Erker, G.; Fuchs, H.; Rogach, A. L.; Chi, L. F. *Small* **2005**, *1*, 524−527.
(17) Huang, J. X.; Kim, F.; Tao, A. R.; Connor, S.; Yang, P. D. *Nat. Mater.* **2005**, *4*, 896−900.
(18) Huang, J. X.; Tao, A. R.; Connor, S.; He, R. R.; Yang, P. D. *Nano Lett.* **2006**, *6*, 524−529.
(19) Lu, N.; Chen, X. D.; Molenda, D.; Naber, A.; Fuchs, H.; Talapin, D. V.; Weller, H.; Muller, J.; Lupton, J. M.; Feldmann, J.; Rogach, A. L.; Chi, L. F. *Nano Lett.* **2004**, *4*, 885−888.
(20) Chen, X. D.; Rogach, A. L.; Talapin, D. V.; Fuchs, H.; Chi, L. F. *J. Am. Chem. Soc.* **2006**, *128*, 9592−9593.
(21) Talapin, D. V.; Rogach, A. L.; Kornowski, A.; Haase, M.; Weller, H. *Nano Lett.* **2001**, *1*, 207−211.
(22) Chen, X. D.; Hirtz, M.; Fuchs, H.; Chi, L. F. *Adv. Mater.* **2005**, *17*, 2881−2885.
(23) Israelachvili, J. *Intermolecular and Surface Forces*; Academic Press: San Diego, CA, 1991.
(24) Owens, D. K.; Wendt, R. C. *J. Appl. Polym. Sci.* **1969**, *13*, 1741−1747.

NL072069B